

Supplementary information

A Variable-Stiffness and Healable Pneumatic Actuator

Hong-Qin Wang[#], Zi-Yang Huang[#], De-Wei Yue, Fang-Zhou Wang, Cheng-Hui Li^{*}

State Key Laboratory of Coordination Chemistry, School of Chemistry and Chemical Engineering, Nanjing National Laboratory of Microstructures, Collaborative Innovation Center of Advanced Microstructures, Nanjing University, Nanjing 210023, P. R. China.

***Corresponding author.** E-mail: chli@nju.edu.cn

[#]Equally contributed to this work.

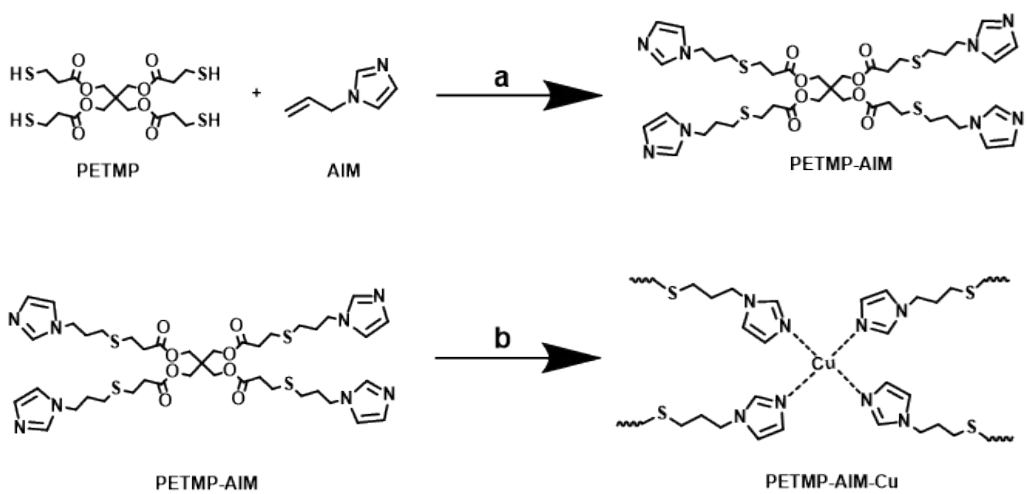


Fig. S1. Synthesis of the highly cross-linked PETMP-AIM-Cu polymer. (a) DMPA, THF, 365nm, rt; ¹ (b) $\text{Cu}(\text{BF}_4)_2 \cdot 6\text{H}_2\text{O}$, EtOH.

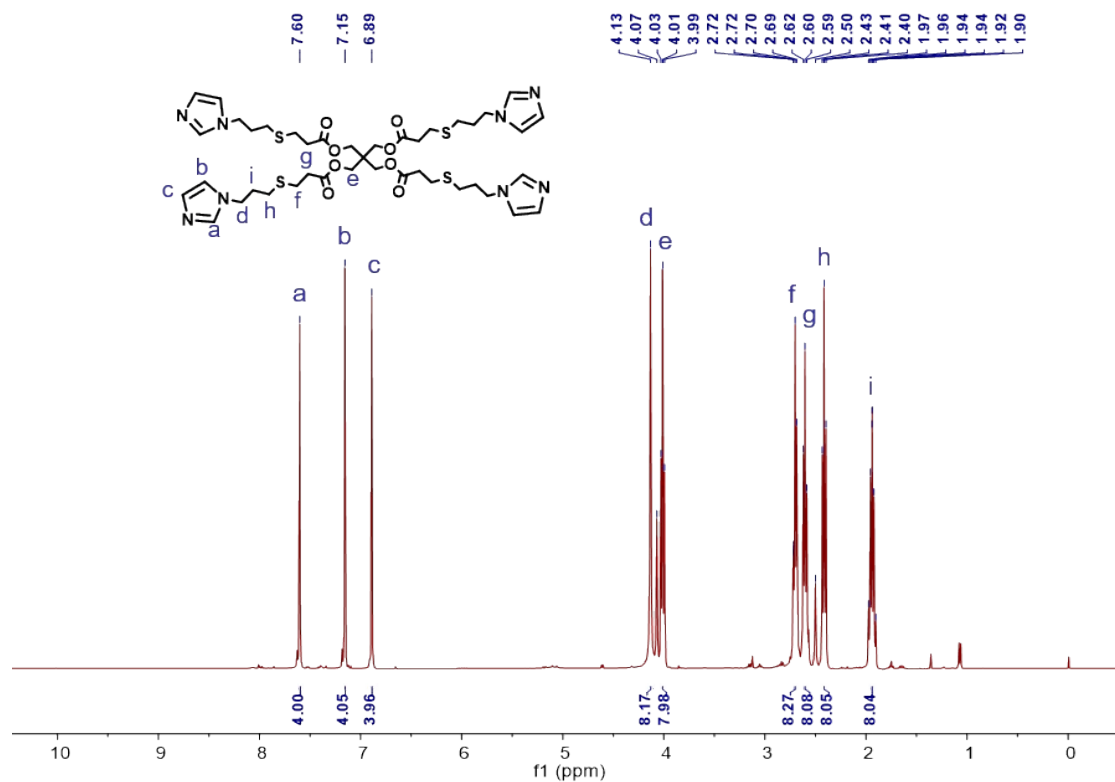


Fig. S2. ¹H NMR spectra of compound PETMP-AIM (500MHz, $\text{DMSO}-d_6$).

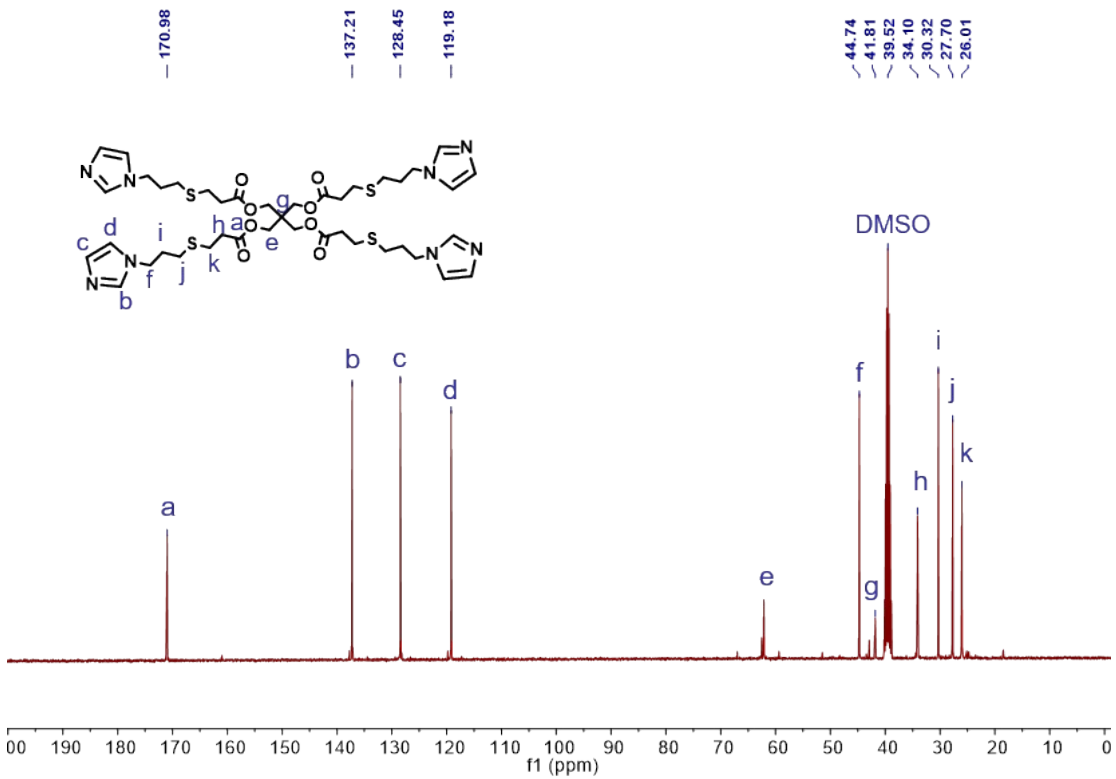


Fig. S3. ^{13}C NMR spectra of compound PETMP-AIM (125MHz, DMSO- d_6).

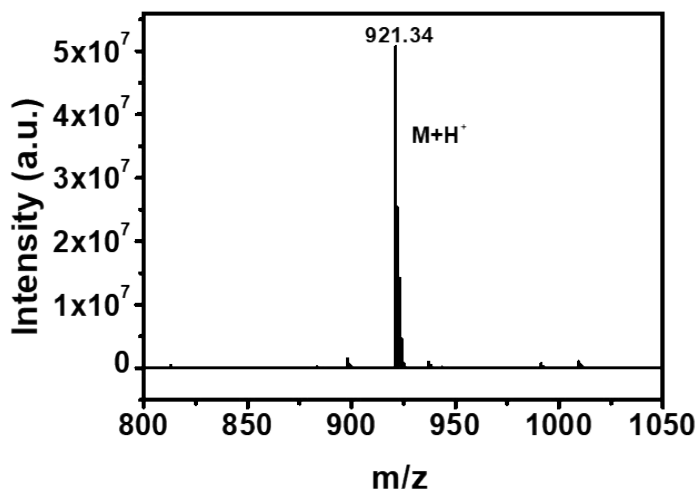


Fig. S4. ESI-MS spectrum for PETMP-AIM.

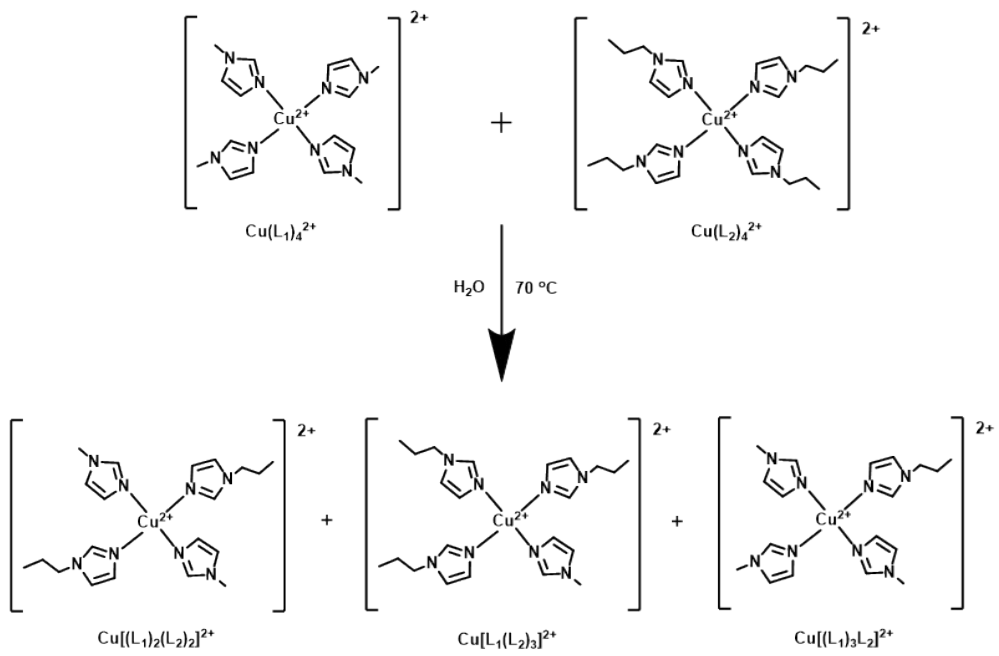


Fig. S5. Ligand exchange process in the small model molecule complexes.

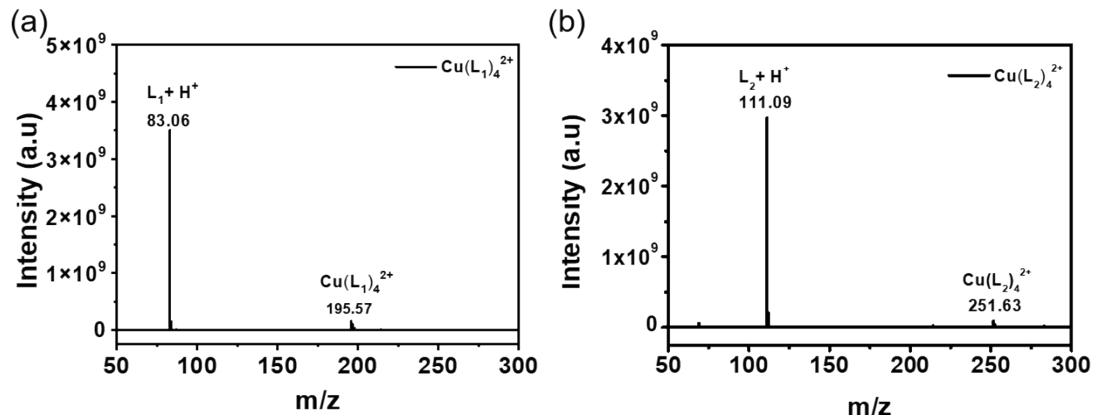


Fig. S6. ESI-MS spectrum for (a) $\text{Cu}(\text{L}_1)_4(\text{BF}_4)_2$ and (b) $\text{Cu}(\text{L}_2)_4(\text{BF}_4)_2$.

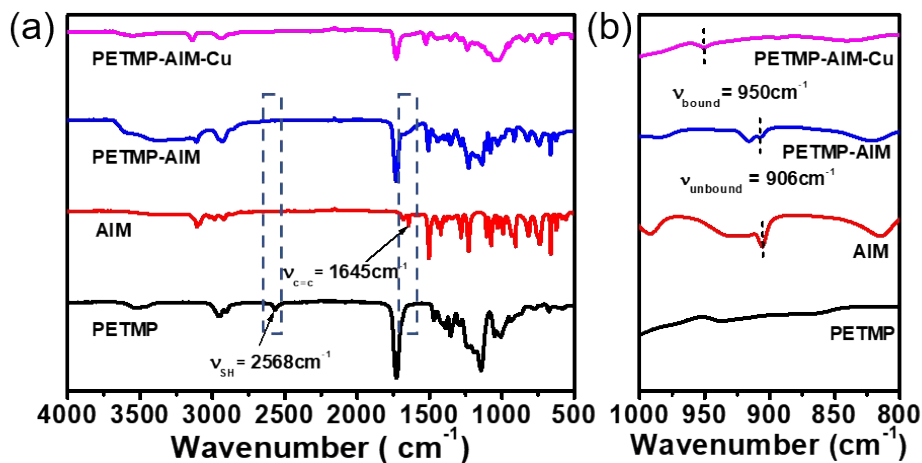


Fig. S7. FT-IR spectra of PETMP, AIM, PETMP-AIM, PETMP-AIM-Cu. (a) The disappearance of stretching vibration at 2568 cm^{-1} of -SH and 1645 cm^{-1} of C=C also confirmed the successful synthesis of PETMP-AIM. (b) The characteristic vibration peak of the imidazole ring at 906 cm^{-1} in PETMP-AIM disappeared, and the coordination of Cu(II) and imidazole appeared at 950 cm^{-1} in PETMP-AIM-Cu.²

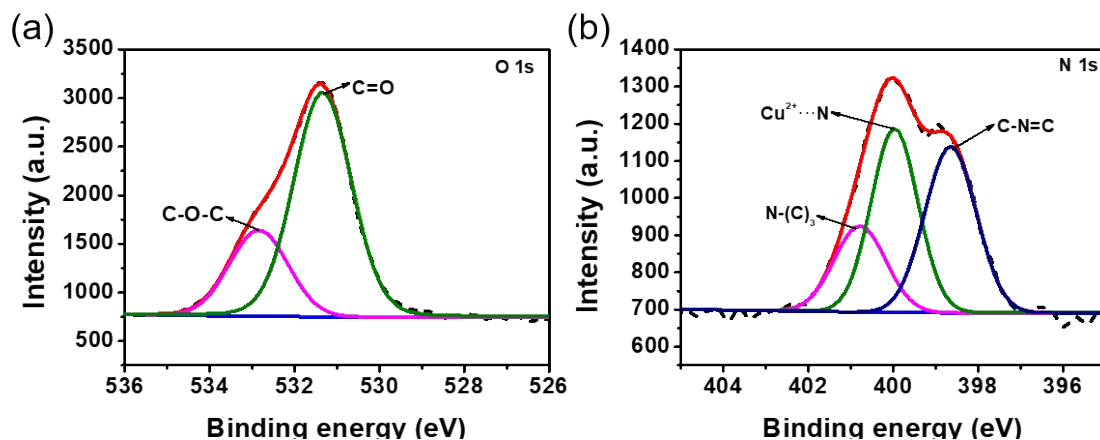


Fig. S8. O 1s and N 1s spectra of PETMP-AIM-Cu. The $\text{Cu}^{2+}\cdots\text{N}$ (399.97 eV , N 1s spectrum) could be easily distinguished from the deconvoluted peaks in the XPS spectra of PETMP-AIM-Cu, in agreement with FT-IR results.³⁻⁶

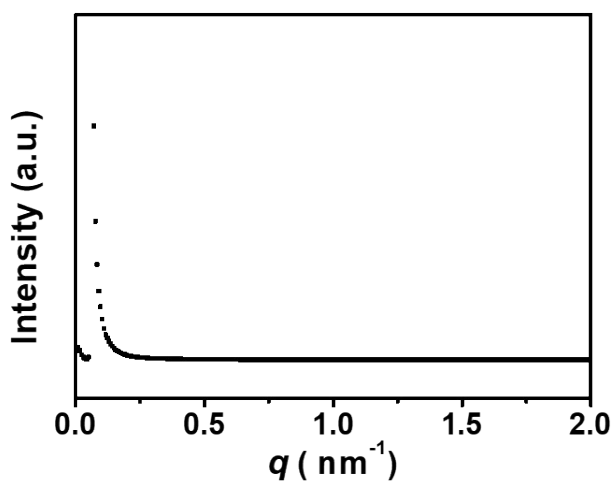


Fig. S9. SAXS spectrum of PETMP-AIM-Cu.

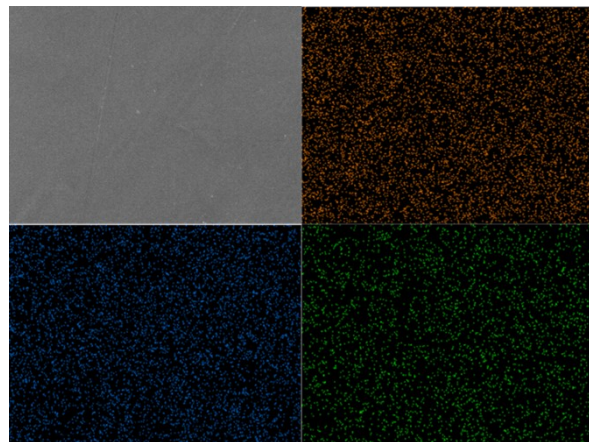


Fig. S10. EDS spectra of PETMP-AIM-Cu.

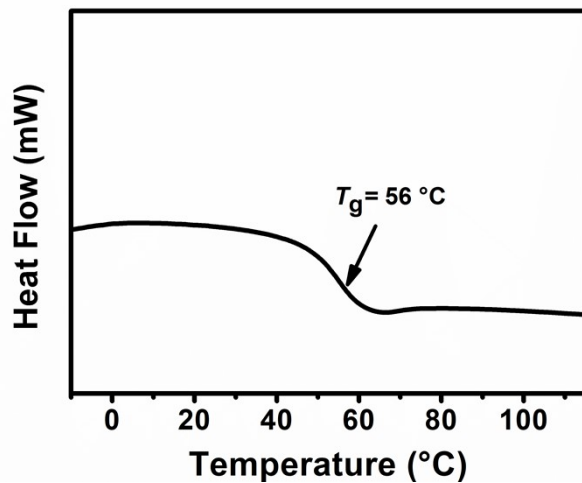


Fig. S11. DSC curve of PETMP-AIM-Cu.

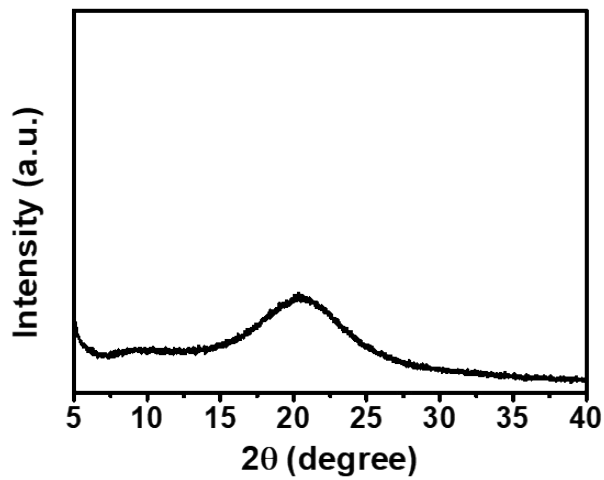


Fig. S12. XRD spectrum of PETMP-AIM-Cu.

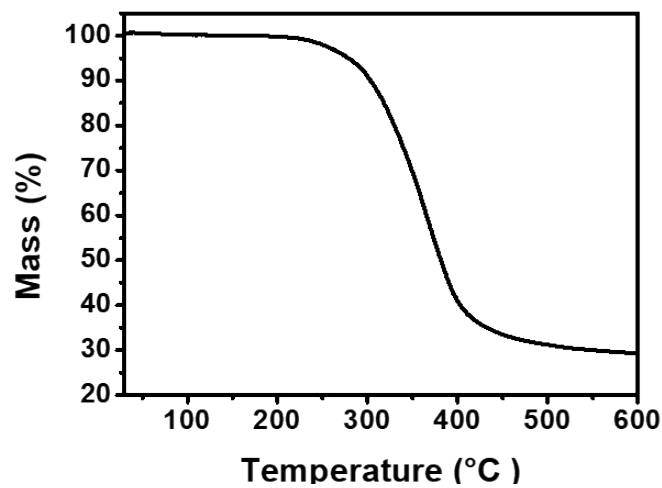


Fig. S13. TGA curve of PETMP-AIM-Cu.

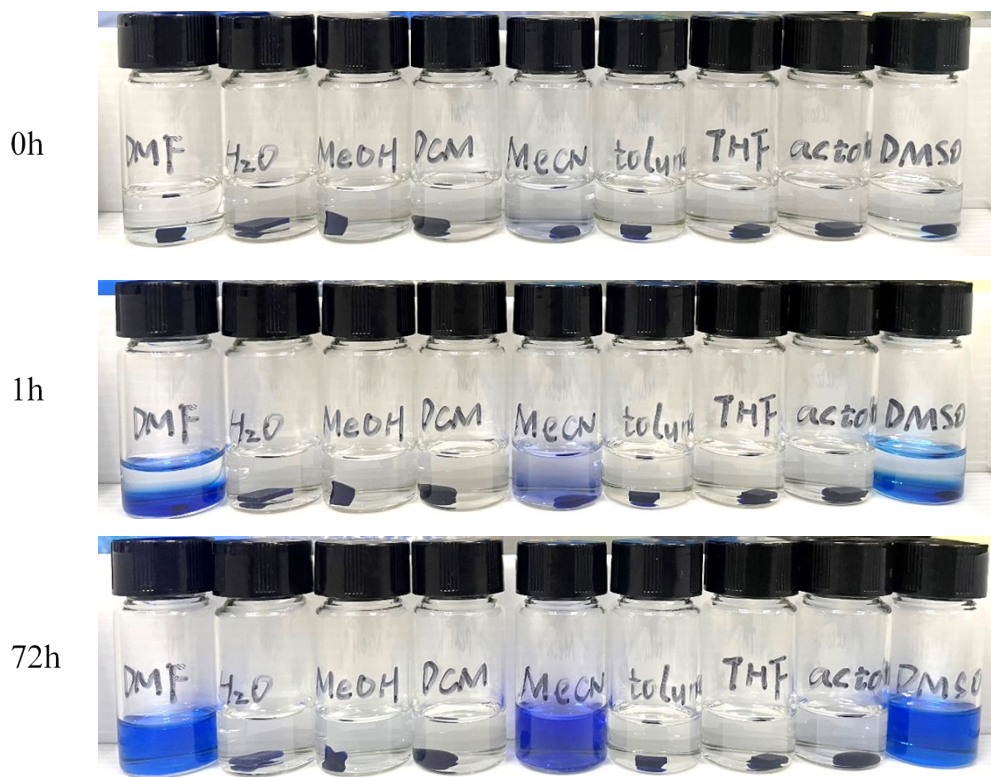


Fig. S14. The dissolution experiments for IPETMP-AIM-Cu at room temperature. It shows that the polymer slightly swells in H₂O, methanol, dichloromethane, toluene, tetrahydrofuran and acetone, dissolve in dimethylformamide, acetonitrile and dimethyl sulfoxide.

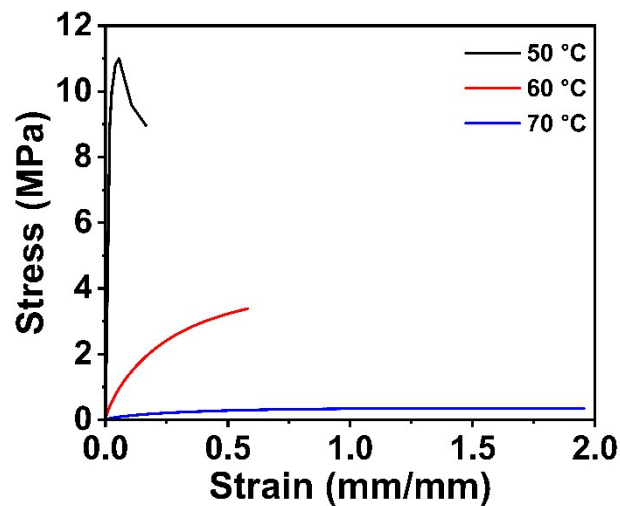


Fig. S15. Tensile stress-strain curves of PETMP-AIM-Cu under various temperature.

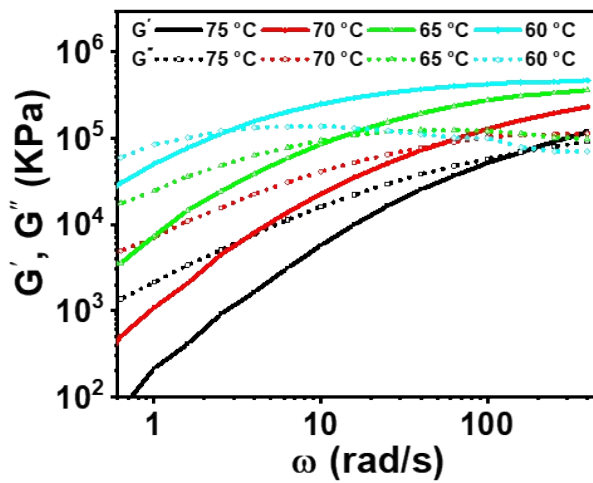


Fig. S16. Frequency-sweep rheology results at different temperature of PETMP-AIM-Cu.

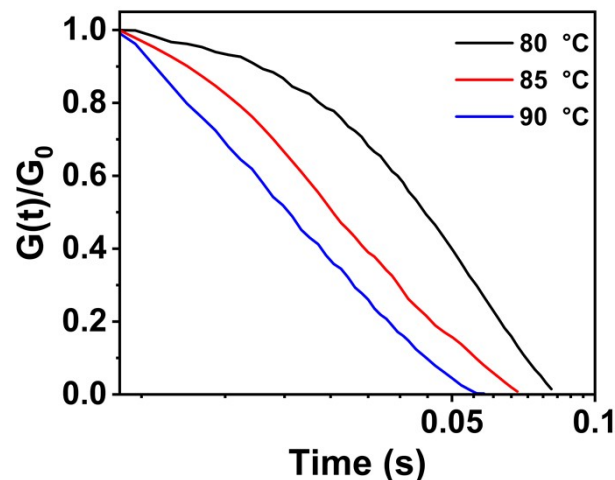


Fig. S17. Temperature-dependent stress relaxation for PETMP-AIM-Cu. the stress relaxation tests for PETMP-AIM-Cu was conducted ranging from 80 °C to 90 °C upon applying a 1% shear stain to the material and recording the shear modulus decay overtime. As we can see from the data, the network behaves dynamically in response to increased temperature and rapid stress relaxation occurred at high temperature which was originated from the reduction in crosslinking densities due to the dissociation of the coordination bonds.

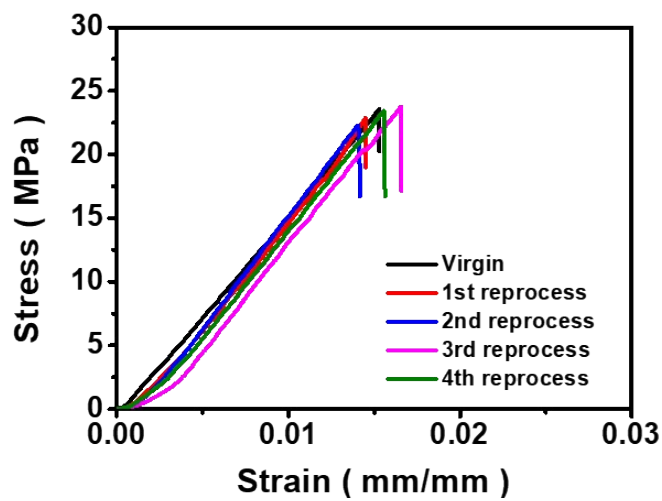


Fig. S18. Reprocessing performance of PETMP-AIM-Cu.



Fig. S19. 3D printing for PETMP-AIM-Cu polymer.

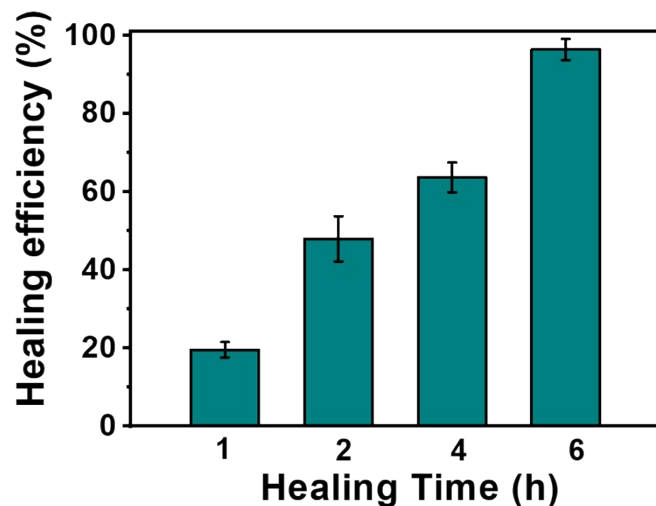
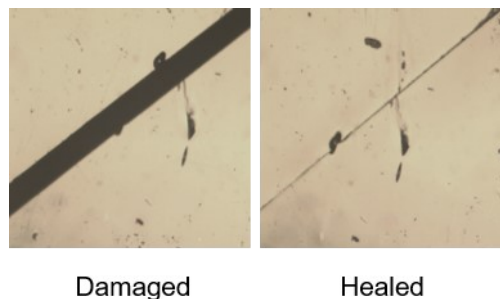


Fig. S20. The self-healing efficiency of PETMP-AIM-Cu for different durations at 70 °C.



Damaged Healed

Fig. S21. Optical microscopic images before (the left) and after (the right) healing at 70 °C for 6 h. Scale bar, 100 μ m.

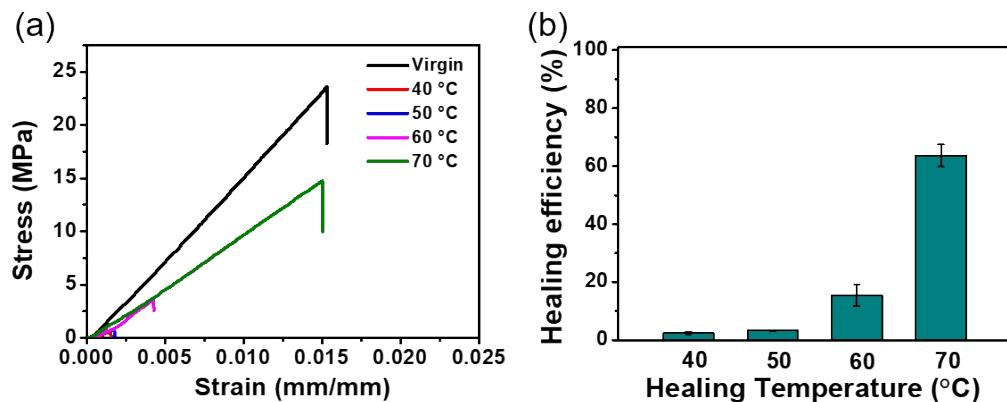


Fig. S22. Flexural stress-strain curves (a) and the self-healing efficiency (b) of PETMP-AIM-Cu at different temperatures for 4 h.

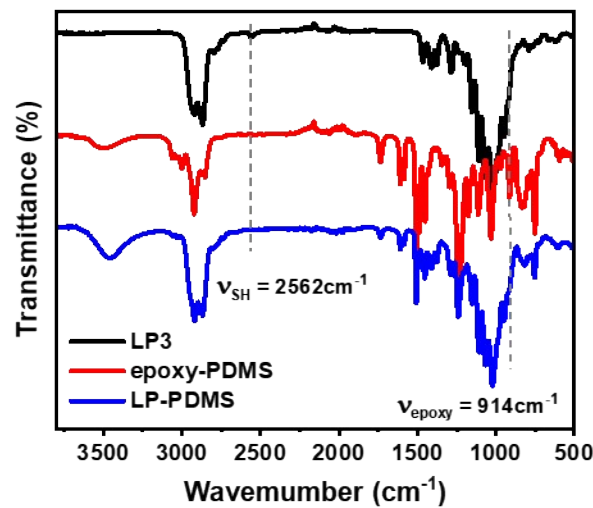


Fig. S23. FT-IR spectra of LP3, epoxy-PDMS, LP-PDMS. The disappearance of stretching vibration at 2568 cm^{-1} of LP3 and 914 cm^{-1} of epoxy-PDMS also confirmed the successful synthesis of LP-PDMS.

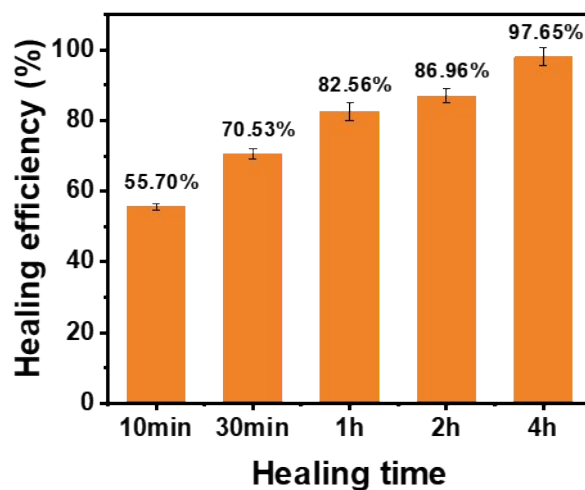


Fig. S24. The self-healing efficiency of LP-PDMS elastomer for different duration at 70 °C.

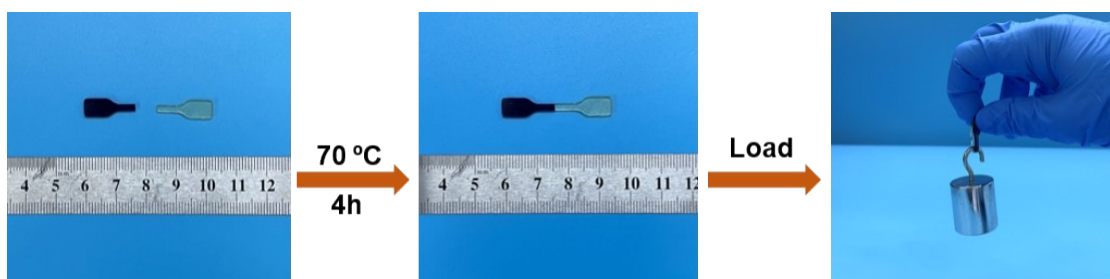


Fig. S25. Photographs of self-healing between either two freshly cut surfaces (yellow and blue) of samples at the temperature of 70 °C for 4 h.

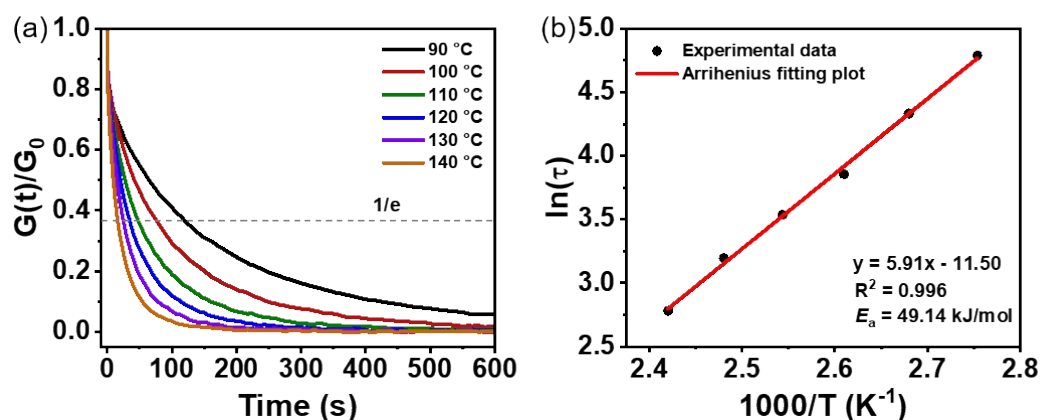


Fig. S26. Dynamic mechanical behaviour of the LP-PDMS elastomer. (a) Normalized stress relaxation curves of the LP-PDMS elastomer. The measurements were performed at a shear strain of 2% at different temperatures from 90 °C to 140 °C. (b) Arrhenius fitting plots of the LP-PDMS elastomer.

Table S1. Results of ITC of the PETMP-AIM (0.3 mM, in cell) with Cu(BF₄)₂·6H₂O (0.15 mM, in syringe) in anhydrous ethanol at 25 °C.

Model	Variable	Value
One sites	K _a (M ⁻¹)	1.78×10 ⁶ ± 4.80×10 ⁵
	N	1.10 ± 0.00545
	ΔH (kJ mol ⁻¹)	-2.468×10 ⁴ ± 290.2
	ΔS (J mol ⁻¹ K ⁻¹)	-52.1

Table S2. Flexural stress-strain results of PETMP-AIM-Cu for reprocessing.

Reprocess	Flexural modulus (MPa, mean ± s.d., n=3)	Strain (mm/mm, mean ± s.d., n=3)	Bending stress (MPa, mean ± s.d., n=3)
Original	1859 ± 178	1.52 ± 0.05	23.58 ± 3.09
1	1743 ± 78	1.45 ± 0.56	22.86 ± 2.43
2	1822 ± 92	1.42 ± 0.02	22.30 ± 2.72
3	1765 ± 164	1.65 ± 0.17	23.77 ± 4.58
4	1715 ± 169	1.55 ± 0.07	23.43 ± 6.42

Table S3. Quantitative analysis of stiffness-variable material for thermal induced stiffness variable polymers reported in literature.

Entry	Material	Temperature Range (°C)	$G'_{\max} \sim G'_{\min}$ or $E'_{\max} \sim E'_{\min}$	σ	Ref.
1	PDMS-COO-Zn	25 – 125	470 MPa – 0.06 MPa	8000	7
2	EGTPA	25 – 125	440 MPa – 0.0084 MPa	50000	8
3	SMP	25 – 70	1 GPa – 10 MPa	1000	9
4	Thermoplastic polymer	30 – 80	1.02 GPa – 13.5 MP	76	10
5	Wax	25 – 70	200 kPa – 101 kPa	2	11
6	PVAc	25 – 56	1.8 GPa – 0.39 MPa	4615	12
7	LCE	25 – 80	1 MPa – 5 kPa	200	13
8	FM/epoxy composite	35 – 70	3.3 GPa – 2.2 MPa	1500	14
9	PADA-5	25 – 130	1.23 MPa – 0.41 MPa	3	15
10	PTBA	25 – 70	1.5 GPa – 0.42 MPa	3571	16
11	BC-BSEP-3	25 – 50	900 MPa – 38 kPa	24000	17
12	LMPA	25 – 50	0.86 GPa – 95.2 kPa	9033	18
13	cPBE	25 – 75	37 MPa – 1.5 MPa	27	19
14	CNF/EG-UPy ₂₉ /SWNT	25 – 150	4GPa – 2.3 GPa	0.43	20
15	PETMP-AIM-Cu	30 – 120	621 MPa – 190 Pa	3268000	This work

Table S4. The self-healing efficiency of PETMP-AIM-Cu for different durations at 70 °C.

Healing time (70 °C, h)	Maximal strength (MPa, mean ± s.d., n=3)	Healing efficiency (MPa, mean ± s.d., n=3)
Original	23.58	-
1	4.55 ± 0.46	19.54 ± 1.96
2	11.30 ± 1.36	47.9 ± 5.78
4	14.75 ± 0.77	62.55 ± 3.82
6	22.72 ± 0.63	96.38 ± 2.71

Table S5. The self-healing efficiency of PETMP-AIM-Cu at different temperatures for 4 h.

Healing temperature (4h, °C)	Maximal strength (MPa, mean ± s.d., n=3)	Healing efficiency (MPa, mean ± s.d., n=3)
Original	23.58	-
40	0.56 ± 0.13	2.41 ± 0.56
50	0.80 ± 0.03	3.39 ± 0.15
60	3.62 ± 0.86	15.39 ± 3.65
70	14.75 ± 0.77	62.55 ± 3.82

Reference

- 1 J. Shi, N. Zhao, D. Yan, J. Song, W. Fu and Z, Li, *J. Mater. Chem. A*, 2020, **8**, 5943-5951.
- 2 J. A. Welleman, F. B. Hulsbergen, J. Verbiest and J. Reedijk, *J. Inorg. Nucl. Chem.*, 1978, **40**, 143-147.
- 3 Y. J. Kim and C. R. Park, *Inorg. Chem.*, 2002, **41**, 6211-6216.
- 4 G. P. López, D. G. Castner and B. D. Ratner, *Surf. Interface Anal.*, 1991, **17**, 267-272.

- 5 G. Xue, Q. Dai and S. Jiang, *J. Am. Chem. Soc.*, 1988, **110**, 2393-2395.
- 6 J. Xu, W. Chen, C. Wang, M. Zheng, C. Ding, W. Jiang, L. Tan and J. Fu, *Chem. Mater.*, 2018, **30**, 6026-6039.
- 7 J. -C. Lai, L. Li, D. -P. Wang, M. -H. Zhang, S. -R. Mo, X. Wang, K. -Y. Zeng, C. -L. Li and J. -L. Zuo, *Nat. Commun.*, 2018, **9**, 1-9.
- 8 M. -H. Zhang, C. -H. Li and J. -L. Zuo, *Cell Rep. Phys. Sci.*, 2020, **1**, 100144.
- 9 Y. -F. Zhang, N. Zhang, H. Hingorani, N. Ding, D. Wang, C. Yuan, B. Zhang, G. Gu and Q. Ge, *Adv. Funct. Mater.*, 2019, **29**, 1806698.
- 10 A. Balasubramanian, M. Standish and C. J. Bettinger, *Adv. Funct. Mater.*, 2014, **24**, 4860-4866.
- 11 N. G. Cheng, A. Gopinath, L. Wang, K. Iagnemma and A. E. Hosoi, *Macromol. Mater. Eng.*, 2014, **299**, 1279-1284.
- 12 J. R. Capadona, K. Shanmuganathan, D. J. Tyler, S. J. Rowan and C. Weder, *Science*, 2008, **319**, 1370-1374.
- 13 T. J. White and D. J. Broer, *Nat. Mater.*, 2015, **14**, 1087-1098.
- 14 T. L. Buckner, M. C. Yuen, S. Y. Kim and R. Kramer-Bottiglio, *Adv. Funct. Mater.*, 2019, **29**, 1903368.
- 15 W. Hu, Z. Ren, J. Li, E. Askounis, Z. Xie and Q. Pei, *Adv. Funct. Mater.*, 2015, **25**, 4827-4836.
- 16 Z. Yu, W. Yuan, P. Brochu, B. Chen, Z. Liu and Q. Pei, *Appl. Phys. Lett.*, 2009, **95**, 192904.
- 17 Y. Qiu, E. Askounis, F. Guan, Z. Peng, W. Xiao and Q. Pei, *ACS Appl. Polym. Mater.*, 2020, **2**, 2008-2015.
- 18 L. Wang, Y. Yang, Y. Chen, C. Majidi, F. Iida, E. Askounis and Q. Pei, *Mater. Today*, 2018, **21**, 563-576.
- 19 W. Shan, S. Diller, A. Tutcuoglu and C. Majidi, *Smart. Mater. Struct.*, 2015, **24**, 065001.
- 20 D. Jiao, F. Lossada, J. Guo, O. Skarsetz, D. Hoenders, J. Liu and A. alther, *Nat. Commun.*, 2021, **12**, 1-10.